Hindawi
International Journal of Aerospace Engineering
Volume 2022, Article ID 6612864, 15 pages
https://doi.org/10.1155/2022/6612864

Research Article

On High-Dimensional Time-Variant Reliability Analysis with the Maximum Entropy Principle

Fuliang Zhou,[1] Yu Hou,[2] and Hong Nie[1]

[1]*College of Aerospace Engineering, Nanjing University of Aeronautics and Astronautics, Nanjing 210016, China*
[2]*School of Aeronautic Engineering, Nanjing Vocational University of Industry Technology, Nanjing 210023, China*

Correspondence should be addressed to Hong Nie; hnie@nuaa.edu.cn

Received 21 October 2021; Revised 7 January 2022; Accepted 4 February 2022; Published 19 March 2022

Academic Editor: Xingling Shao

The structural reliability analysis suffers from the curse of dimensionality if the associated limit state function involves a large number of inputs. This study develops a reliability analysis method that deals with high-dimensional inputs over time. The probability distribution of the structural response is reconstructed by the maximum entropy principle which is achieved by solving an optimization problem derived from the concept of relative entropy. The optimization problem is transformed into a convex one with respect to the orders of fractional moments and the Lagrange multipliers. Additionally, considering the associated computational issues, it is reformulated with side constraints on the parameters of the maximum entropy distribution. Then, a global optimization procedure is performed. The proposed method is successfully applied to the reliability analysis of a linear and a nonlinear structural system, which involves a large number of inputs deriving from the discretization of the input random processes.

1. Introduction

Structural reliability analysis has been intensively studied during the past few decades. Based on the consideration of time factor, structural reliability analysis can be roughly divided into two groups: time-invariant reliability analysis and time-variant reliability analysis. For the first group, as its name implies, the time-invariant reliability methods do not consider the effect of time factor, for example, first-/second-order reliability method (FORM/SORM) [1–3], moment methods [4, 5], response surface methods [6–9], and importance sampling [10, 11]. Therefore, they only take random variables as inputs. However, almost all structural systems involve time-dependent parameters during their period of operation and/or service, e.g., stochastic loading and material property degradation. Thus, time-invariant reliability analysis may provide inaccurate reliability assessment and prediction.

In the past decade, time-variant reliability analysis has drawn much more attention than its counterpart because of its capacity of dealing with time factor. Thus, the corresponding time-variant reliability methods can take random variables, random processes, and even random fields as inputs. Many time-variant reliability methods have been developed in recent years. They can be roughly classified into three categories: (1) the out-crossing-rate-based methods [12–18], (2) the extreme value methods [19–27], and (3) the composite limit state methods [28–32]. A common feature of these methods is that a time-variant reliability analysis problem is usually transformed into a time-invariant one or broken down into a series of time-invariant ones. Then, the aforementioned time-invariant reliability methods are applied to complete the time-variant reliability analysis. For instance, FORM has been integrated into many time-variant reliability methods [14, 17]. Note that the time-variant reliability methods with FORM inherent the drawbacks of FORM.

Many challenges are encountered by time-variant reliability analysis. One main challenge arises from the curse of dimension when a large number of random variables are used to represent the input random processes and/or fields. It should be pointed out that there is also a universal and

dimension-free tool for both time-invariant reliability analysis and time-variant ones. It is direct Monte Carlo simulation (MCS). However, MCS suffers from a huge computational effort for estimating a small failure probability when a time-consuming model or experiment is involved, e.g., a large-scale finite element model. Subset simulation [33, 34] is an alternative for MCS for estimating small failure probabilities in both time-invariant reliability analysis and time-variant ones. However, several thousands of samples are still required to obtain a robust and accurate estimation by subset simulation.

In this paper, we are interested in developing an efficient and accurate method for high-dimensional time-variant reliability analysis. The high-dimensional issue is solved through the development of a reliability method using statistical moments.

Zhao and Ono's moment method is the most attractive one for structural reliability analysis [4, 5] after the year 2000, where the first three or four moments of structural response are used to fit a parametric distribution. The Pearson system [35] was recommended as the reliability index for the moment method. Although the Pearson system of frequency curves is flexible, they still impose spurious information on the unknown distribution. It is also contentious from both theoretical and practical views [36, 37]. The maximum entropy (MaxEnt) principle was pioneered by Jaynes [38, 39], which minimizes the amount of prior information built into the approximate distribution while maximizing entropy, i.e., a measure of uncertainty. Using the MaxEnt principle, Li and Zhang proposed a combined method for structural reliability analysis [37]. The statistical moments of structural response are calculated by the dimension reduction method [40, 41]. Zhang and Pandey analyzed two challenging issues of using integer moments when approximating the unknown distribution by the MaxEnt principle [36]. They are a large number of required moments and the oscillatory phenomena at the tail of MaxEnt distribution. The usage of fractional moments [42] was proposed to overcome these two issues for time-invariant reliability problems since a fractional moment contains the statistical information of a large number of integer moments. A multiplicative dimensional reduction method was also developed to compute the fractional moments of structural response [36]. Considering correlated input random variables, Li et al. suggested using the unscented transformation technique to calculate fractional moments [43]. Dai et al. employed the MaxEnt principle to construct the optimal importance sampling density for the importance sampling method [44]. However, the above investigations are limited to time-invariant reliability problems.

For the time-variant reliability analysis problem, Shi et al. presented the performance of the combination of dimension reduction method and the MaxEnt principle with fractional moments [45]. Xu and his colleagues carried out a series of studies about the MaxEnt principle with fractional moments and their applications for time-variant reliability analysis [46–50]. However, the number of input random variables in the application examples is not beyond 20 [45–50]. Thus, the abovementioned methods cannot be applied to the time-variant reliability analysis problems involving a large number of inputs [47].

The objective of this paper is to propose an efficient method for the high-dimensional time-variant reliability problems by using the MaxEnt principle with fractional moments, where the number of input random variables is larger than 100. The contributions of this study are as follows: (1) a new perspective for estimating a failure probability curve from the combination of fractional moments and the maximum entropy principle and (2) a new tool for high-dimensional and nonlinear time-variant reliability analysis with input random variables and processes. High-dimensional issue is very challenging in many science and engineering fields [51–53]. To address this issue, fractional moment and the maximum entropy distribution are used to approximate the probability density function of structural responses of interested, which has a capacity of dealing with zero-shot events [54] for structural reliability analysis. In other words, the proposed method can estimate structural reliability with zero-failure samples.

The remainder of the paper is organized as follows: Section 2 briefly reviews the problem setup for time-variant reliability analysis. Section 3 describes the procedure and theoretical rationale of the proposed method. Section 4 analyzes the implementation issues and their corresponding possible solutions. Two high-dimensional examples are used to demonstrate the performance of the proposed method in Section 5. Concluding remarks are provided in Section 6.

2. Problem Statement

Limit state functions (LSFs) are employed to capture the intended operating condition of structures in the structural reliability community, which divides the operating space into two domains, i.e., the safe domain and the failure domain. Let $g(\cdot)$ be an LSF of the intended operating condition of a structure, where $g(\cdot) > 0$ indicates the structure is safe while $g(\cdot) \le 0$ means there is a failure in the structure. The general form of LSF is defined as

$$G = g(\mathbf{X}, \mathbf{Y}(t), t), \tag{1}$$

where G is the response quantity, $\mathbf{X}$ is the input random variable vector, $\mathbf{Y}(t)$ is the input random process vector, and t is the input time, respectively. Based on the different type of inputs in the LSF $g(\cdot)$, the LSF may degrade into simpler types [22]. It is well-known that reliability is a function of time snice the LSF of interest is related to time via the time-dependent random process $\mathbf{Y}(t)$ and the explicit operating time t. Suppose that we are interested in the time-variant reliability of the structure over a time interval $[0, t_f]$, where t_f is the final time instant. The time-variant reliability $R(0, t_f)$ can be expressed as

$$R(0, t_f) = \Pr\left\{G = g(\cdot) > 0, \forall t \in [0, t_f]\right\}, \tag{2}$$

where the symbol $\forall$ means for all time instants. In practical estimation, the corresponding time-variant failure probability $P_f(0, t_f)$ is more preferable which is defined as a complementary quantity to the time-variant reliability, i.e.,

$$P_f(0, t_f) = \Pr\left\{G = g(\cdot) \le 0, \exists t \in [0, t_f]\right\}, \tag{3}$$

where the symbol $\exists$ has a meaning of "there exists at least one." To distinguish the failure probability over a time interval from that for a time instant, $P_f(0, t_f)$ in Equation (3) is also called as the cumulative failure probability. Obviously, it is a function of the final time t_f.

To handle the input random processes, the time interval of interest $[0, t_f]$ is usually divided into a set of discrete time instants with a constant time step Δt. Let $t_i = i\Delta t$ represent the time instant at the ith step, where the index $i = 1, \cdots, n$. Spectral decomposition methods are suggested to deal with the input random processes and transform them into a set of random variables [17, 22, 24, 26]. Let $\mathbf{Z}$ be the transformed random variables from the input random processes. Then, the LSF becomes $G = g(\mathbf{X}, \mathbf{Z}, t)$. Furtherly, at a time instant t_i, an instantaneous LSF is defined as $G_i = g(\mathbf{X}, \mathbf{Z}, t_i)$. Using the concept of series-system reliability, the cumulative failure probability in Equation (3) is approximated as

$$\begin{aligned} P_f(0, t_f) &\approx \Pr\left\{\bigcup_{i=1}^{n} g(\mathbf{X}, \mathbf{Z}, t_i) \le 0\right\} = \Pr\left\{\bigcup_{i=1}^{n} G_i \le 0\right\} \\ &= \Pr\left\{\max_{i=0,1,\cdots,l}(G_i) \le 0\right\}, \end{aligned} \tag{4}$$

where $W = \max_{i=0,1,\cdots,n}(G_i)$. The advantage of Equation (4) is that the output random process $G = g(\cdot)$ is converted into a random variable W.

The magnitude of time step size Δt affects the approximate accuracy of input random processes with a finite number of random variables firstly. Then, this effect may propagate into Equation (4) through the LSF and furtherly influence the estimation accuracy of the cumulative failure probability. In this study, we assume that the magnitude of time step size is sufficiently small and adequate to capture the uncertainty in the input random processes and failure information in the transformed series system. The current study focuses on the development of a new high-dimensional time-variant reliability analysis method based on Equation (4).

3. Proposed Method

3.1. Overview. The new high-dimensional time-variant reliability analysis method has three stages. The first stage is to generate random samples for the input random variables and random processes using MCS sampling strategy and furtherly compute the structural responses. The second stage involves the approximation of the MaxEnt distribution. The third stage is related to the calculation of failure probability using the MaxEnt distribution obtained in the second stage. It is clear that the second stage is the key stage of the proposed method. The implementation procedure of the proposed method is shown in Figure 1.

Stage 1 involves four steps. Step 1: discretize the time interval $[0, t_f]$ with a constant time step size Δt and obtain $n+1$ discrete time instant $(t_0 = 0, t_1, \cdots, t_n = t_f)$. Step 2: decompose the input random processes $\mathbf{Y}(t)$ with a group of random variables $\mathbf{Z}$. Step 3: generate N random samples for the input random variables and random processes. Step 4: substitute the random samples into the LSF to obtain N trajectories of structural response.

Stage 2 is furtherly divided into three steps. Step 1: solve the optimization problem derived from the concept of relative entropy. Step 2: calculate the fractional moments from the N trajectories of structural response. Step 3: determine the MaxEnt distribution based on the solution to the optimization problem in Step 1. In the subsequent sections, we will discuss the details of Step 1 and 3 since these steps are theoretical fundamentals of the proposed method.

Stage 3 is straightforward once the probability density function (PDF) of MaxEnt distribution is determined in Stage 2. The estimation of a cumulative failure probability is just a numerical integration over the failure domain.

3.2. Maximum Entropy Principle with Fractional Moments. The advantages of usage of fractional moments in the maximum entropy principle have been proven by several studies in the structural reliability community [36, 43, 45–50]. This subsection will give a brief review of the maximum entropy principle with fractional moments.

Identifying the probability distribution with statistical moments has been investigated extensively in the literature. However, the use of integer statistical moments suffers from accuracy concern. Zhang and Pandey study the need of fractional moments instead of integer moments, which is evoked by the relationship between them [36].

We start with the definition of the fractional binomial coefficient $\binom{\alpha}{i}$ that is given by

$$\binom{\alpha}{i} = \frac{\alpha(\alpha-1)\cdots(\alpha-i+1)}{i(i-1)\cdots 1}, \tag{5}$$

where α is a real number and i is an integer number. If applying the Taylor series expansion on a function of x^α, one has

$$x^\alpha = \sum_{i=0}^{\infty}\binom{\alpha}{i} c^{\alpha-i}(x-c)^i, \tag{6}$$

where c is a reference point.

The αth-order fractional moment of a positive random variable X is defined as

$$E[X^\alpha] = \int_X x^\alpha f_X(x)dx. \tag{7}$$

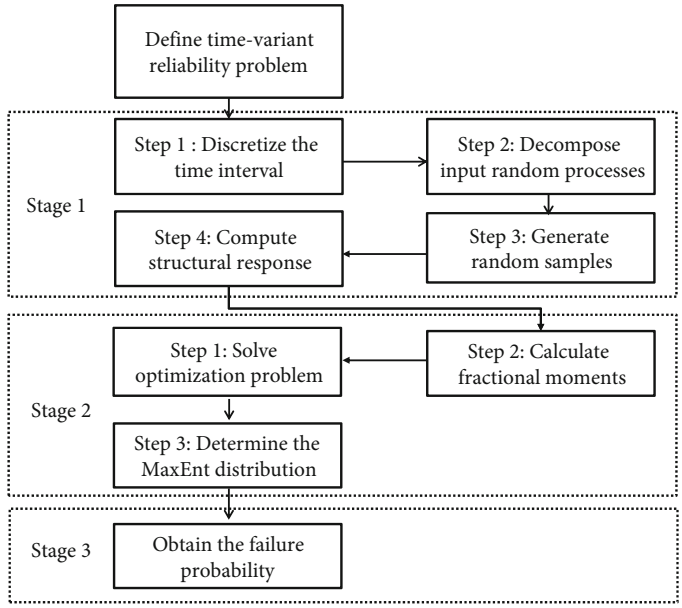

Figure 1: Procedure of the proposed method.

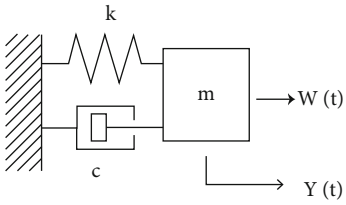

Figure 2: The SDOF oscillator.

Substituting Equation (6) into Equation (7), one has

$$E[X^{\alpha}] = \sum_{i=0}^{\infty} \binom{\alpha}{i} c^{\alpha-i} E\left[(X-c)^{i}\right] \tag{8}$$

where $E[(X-c)^{i}]$ is the ith central moment of the random variable X. If the reference point is put on the mean value of the random variable X, the ith central moment can be rewritten as

$$E\left[(X-c)^{i}\right] = \sum_{k=0}^{i} (-1)^{i-k} \binom{i}{k} c^{i-k} E\left[X^{k}\right], \quad i = 1, 2, \cdots. \tag{9}$$

Equations (8) and (9) indicate that a fractional moment includes the information of a series of integer statistical moments, either central moments or raw moments.

If a couple of fractional moments are available at hand, they would provide much more information than the same number of integer moments for identifying an unknown distribution type. In contrast, Gzyl and Tagliani [55] proved that 30 or more integer moments are required by Equations (8) and (9) to guarantee the accuracy of a fractional moment, where the infinite sequence of integer moments is demanded theoretically. This result is extremely important and gives a strong motivation to employ the concept of the fractional moment to reconstruct an unknown distribution type from a group of samples.

The information entropy of a random variable X is a measure of the uncertainty containing by the random variable, which is defined as

$$H_X = \int f_X(x) \log\left(f_X(x)\right) dx, \tag{10}$$

where $f_X(x)$ is the probability density function of the random variable X.

The core step of the proposed method in this study is to reconstruct an expression for the unknown PDF of the structural response G, given a sample of experimental data. The MaxEnt principle states that the most unbiased estimation of the unknown PDF is the one that maximizes Equation (10) with given constraints. In this study, the given constraints are the fractional moments determined from the experimental data. Therefore, by the MaxEnt principle, the PDF identification problem is converted into an optimization problem [42].

$$\begin{aligned} \max \quad & H_X, \\ s.t. \quad & \int f_X(x) dx = 1, \\ & \int x^{\alpha} f_X(X) dx = M_x^{\alpha}, \end{aligned} \tag{11}$$

where M_x^{α} is the αth fractional moment estimated from a sample

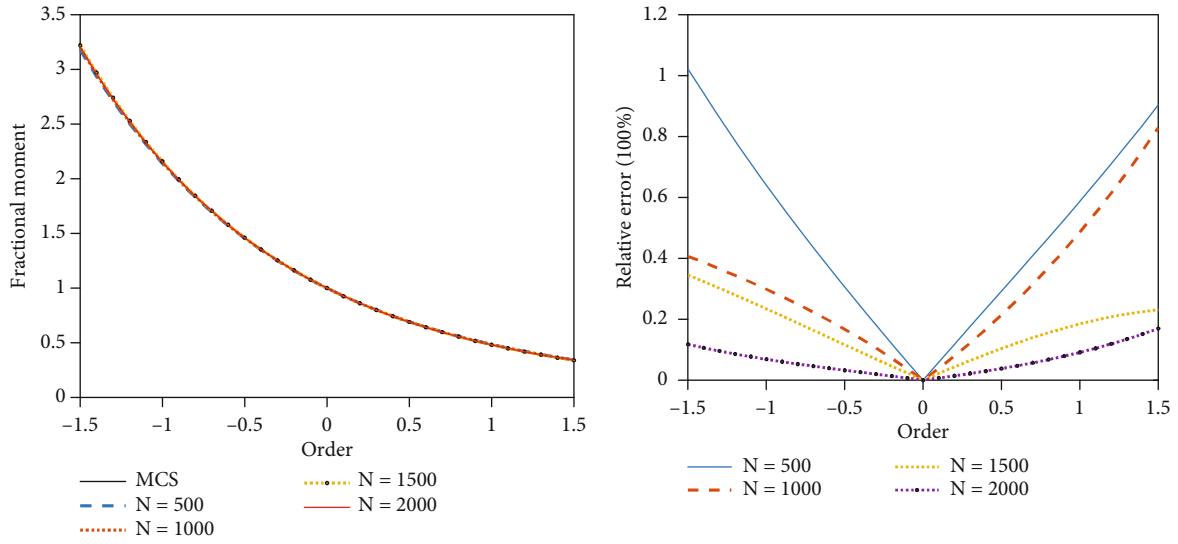

(a) Fractional moment

(b) Relative error

Figure 3: Fractional moments and relative error of the normalized response (the SDOF oscillator).

Table 1: The value of the objective function without penalty term.

	$N = 500$	$N = 1000$	$N = 1500$	$N = 2000$
$m = 3$	0.406786	0.408704	0.398282	0.397276
$m = 4$	0.406792	0.408709	0.398292	0.397279
$m = 5$	0.406797	0.408708	0.398286	0.397281

Table 2: The value of the objective function with penalty term.

	$N = 500$	$N = 1000$	$N = 1500$	$N = 2000$
$m = 3$	0.4128	0.4117	0.4003	0.3988
$m = 4$	0.4148	0.4127	0.4010	0.3993
$m = 5$	0.4168	0.4137	0.4016	0.3998

$$M_x^{\alpha} = \frac{1}{N}\sum_{i=1}^{N} x_i^{\alpha} \approx E[X^{\alpha}]. \tag{12}$$

Note that x_i are the random samples for the random variable X and N is the number of experimental points in the sample.

Solving the optimization problem with the Lagrange multiplier method, one has the following generic form of the MaxEnt distribution [36, 42].

$$\widehat{f}_X(x) = \exp(-\lambda_0)\exp\left(-\sum_{i=1}^{m}\lambda_i x^{\alpha_i}\right), \tag{13}$$

where $\widehat{f}_X(x)$ denotes the MaxEnt PDF for $f_X(x)$, λ_i are the Lagrange multipliers, α_i are the orders for the fractional moments, and m is the number of available fractional moments, respectively. The parameter λ_0 is a normalizing factor which makes sure that the integration of $\widehat{f}_X(x)$ over its support domain is 1 and satisfies the definition of PDF. Thus, from Equation (13), one has

$$\lambda_0 = \log\left[\int \exp\left(-\sum_{i=1}^{m}\lambda_i x^{\alpha_i}\right)\right]. \tag{14}$$

Based on the concept of relative entropy (or the Kullback-Leibler distance), Zhang and Pandey proved that the following optimization problem is equivalent to Equatio (11) [36].

$$\min\ I(\boldsymbol{\lambda}, \boldsymbol{\alpha}) = \log\left(\int_X \exp\left(-\left(\sum_{i=1}^{m}\lambda_i x^{\alpha_i}\right)\right)dx\right) + \sum_{i=1}^{m}\lambda_i M_X^{\alpha_i}. \tag{15}$$

The minimization of the relative entropy means the minimization of the generalized distance between the true PDF $f_X(x)$ and the estimated PDF $\widehat{f}_X(x)$, which is quantified by the information entropy. We will further reformulate the optimization problem in Equation (15) and derive an attractive property of it in the next subsection.

3.3. Computation of Maximum Entropy Distribution. Recalling the equivalent optimization problem in Equation (15), its objective function is furtherly rewritten as

$$\begin{aligned} I(\boldsymbol{\lambda}, \boldsymbol{\alpha}) &= \log\left(\int_X \exp\left(-\left(\sum_{i=1}^{m}\lambda_i x^{\alpha_i}\right)\right)dx\right) + \sum_{i=1}^{m}\lambda_i M_X^{\alpha_i} \\ &= \log\left(\int_X \exp\left(-\left(\sum_{i=1}^{m}\lambda_i x^{\alpha_i} - \sum_{i=1}^{m}\lambda_i M_X^{\alpha_i}\right)\right)dx\right). \end{aligned} \tag{16}$$

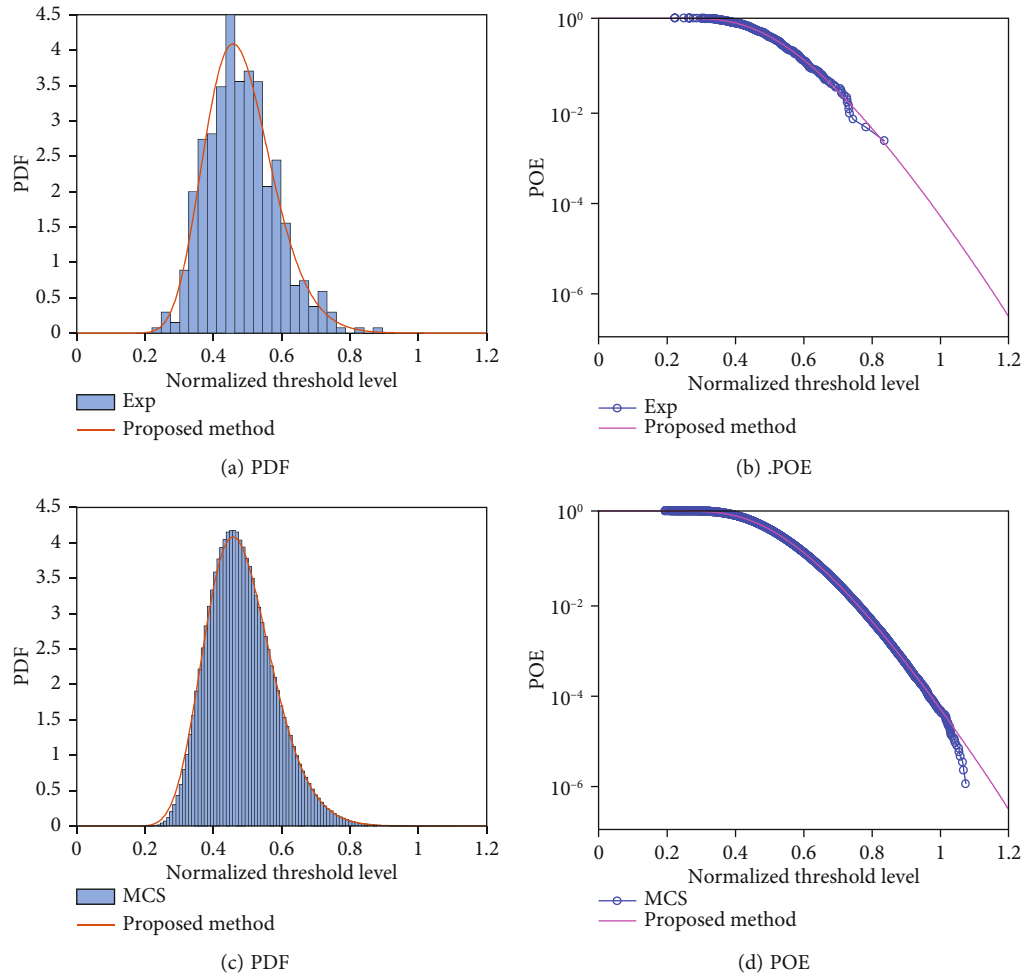

Figure 4: Comparison of histogram, PDF, and POE for $m = 3$ and $N = 500$.

It is obvious that minimizing $\mathrm{I}(\boldsymbol{\lambda}, \boldsymbol{\alpha})$ is equivalent to minimize the following integral:

$$\int_X \exp\left(-\left(\sum_{i=1}^{m}\lambda_i x^{\alpha_i} - \sum_{i=1}^{m}\lambda_i M_X^{\alpha_i}\right)\right)dx \equiv Q(\boldsymbol{\lambda}, \boldsymbol{\alpha}). \quad (17)$$

The integral term is defined as a function $Q(\boldsymbol{\lambda}, \boldsymbol{\alpha})$ for the purpose of simplification. Based on the definition of $Q(\boldsymbol{\lambda}, \boldsymbol{\alpha})$ in Equation (17), the MaxEnt distribution can be rewritten as

$$\widehat{f}(x) = [Q(\boldsymbol{\lambda}, \boldsymbol{\alpha})]^{-1} \exp\left(-\sum_{i=1}^{m}\lambda_i\left(x^{\alpha_i} - M_X^{\alpha_i}\right)\right). \quad (18)$$

This study examines the properties of the integral function $Q(\boldsymbol{\lambda}, \boldsymbol{\alpha})$ firstly. The derivative of $Q(\boldsymbol{\lambda}, \boldsymbol{\alpha})$ with respect to λ_i is written

$$\begin{aligned}\frac{\partial Q}{\partial \lambda_i} &= \int_X \frac{\partial}{\partial \lambda_i}\exp\left(-\left(\sum_{i=1}^{m}\lambda_i x^{\alpha_i} - \sum_{i=1}^{m}\lambda_i M_X^{\alpha_i}\right)\right)dx \\ &= Q(\boldsymbol{\lambda}, \boldsymbol{\alpha})\int_X -\left(x^{\alpha_i} - M_X^{\alpha_i}\right)Q(\boldsymbol{\lambda}, \boldsymbol{\alpha})^{-1}\exp\left(-\left(\sum_{i=1}^{m}\lambda_i x^{\alpha_i} - \sum_{i=1}^{m}\lambda_i M_X^{\alpha_i}\right)\right)dx \\ &= Q(\boldsymbol{\lambda}, \boldsymbol{\alpha})\int_X -\left(x^{\alpha_i} - M_X^{\alpha_i}\right)f_X(x)dx.\end{aligned} \quad (19)$$

Recalling the definition of fractional moment, we have

$$\begin{aligned}\frac{\partial Q}{\partial \lambda_i} &= Q(\boldsymbol{\lambda}, \boldsymbol{\alpha})\int_X -\left(x^{\alpha_i} - M_X^{\alpha_i}\right)f_X(x)dx \\ &= Q(\boldsymbol{\lambda}, \boldsymbol{\alpha})\left(M_X^{\alpha_i} - \int_X (x^{\alpha_i})f_X(x)dx\right) = 0.\end{aligned} \quad (20)$$

The first derivative of $Q(\boldsymbol{\lambda}, \boldsymbol{\alpha})$ with respect to α_i is given by

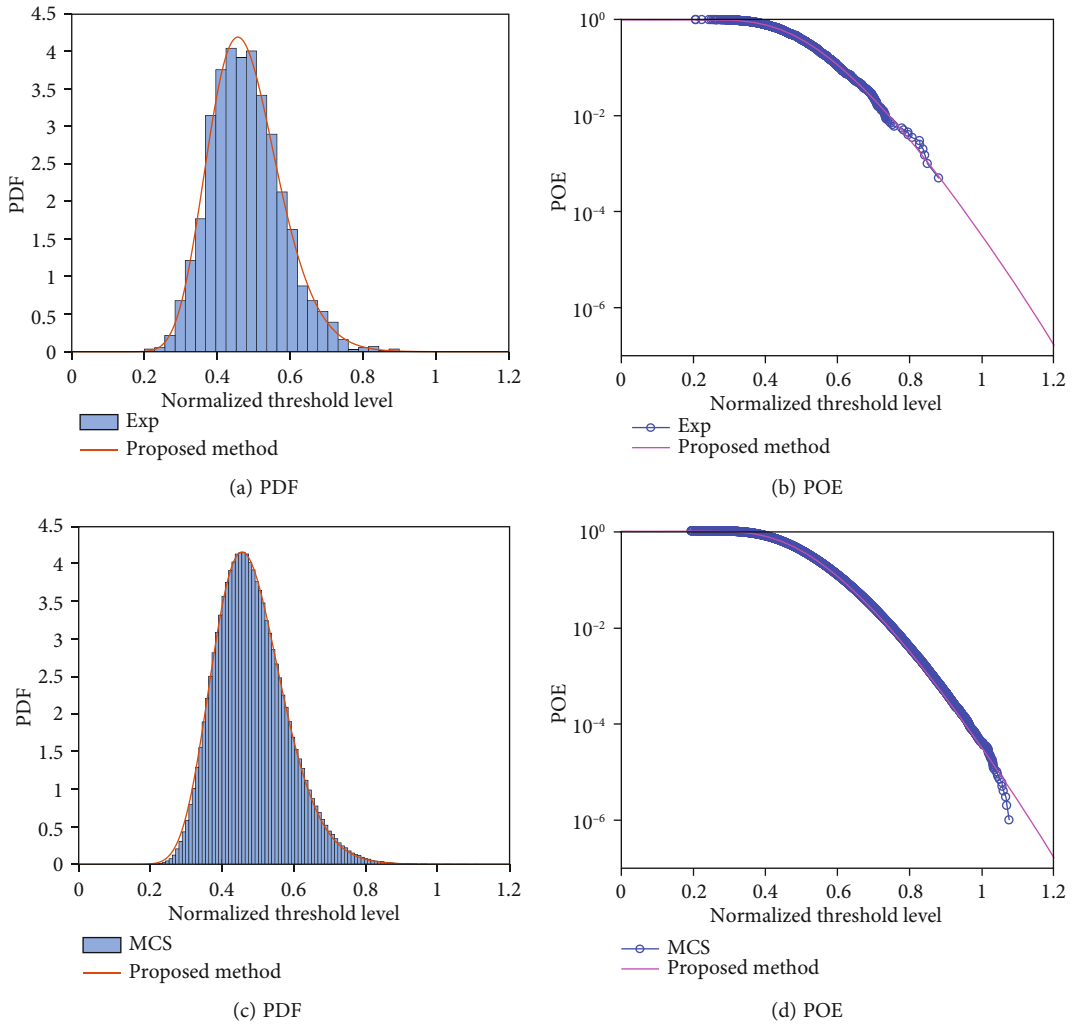

Figure 5: Comparison of histogram, PDF, and POE for $m = 3$ and $N = 2000$.

Table 3: The average computational time of the oscillator example (second).

	$N = 500$	$N = 1000$	$N = 1500$	$N = 2000$
$m = 3$	34.0	41.	34.3	33.4
$m = 4$	23.7	37.4	18.2	30.3
$m = 5$	21.5	22.5	40.0	25.8

$$\begin{aligned}\frac{\partial Q}{\partial \alpha_i} &= \int_X \frac{\partial}{\partial \alpha_i} \exp\left(-\left(\sum_{i=1}^{m}\lambda_i x^{\alpha_i} - \sum_{i=1}^{m}\lambda_i M_X^{\alpha_i}\right)\right) dx \\ &= \int_X -\lambda_i\left(\alpha_i x^{\alpha_i - 1} - \int_X \frac{\partial}{\partial \alpha_i} x^{\alpha_i} f(x) dx\right) \exp\left(-\left(\sum_{i=1}^{m}\lambda_i x^{\alpha_i} - \sum_{i=1}^{m}\lambda_i M_X^{\alpha_i}\right)\right) dx \\ &= Q(\boldsymbol{\lambda}, \boldsymbol{\alpha}) \int_X -\lambda_i \alpha_i \left(x^{\alpha_i - 1} - M_X^{\alpha_i - 1}\right) f_X(x) dx = 0.\end{aligned} \tag{21}$$

From Equations (20) and (21), we know that the solution point $(\lambda_1, \cdots, \lambda_m, \alpha_1, \cdots, \alpha_m)$ to Equation (17) is a saddle point of $Q(\boldsymbol{\lambda}, \boldsymbol{\alpha})$ at least.

Next, we examine the elements in the Hessian matrix of $Q(\boldsymbol{\lambda}, \boldsymbol{\alpha})$. There are four types elements in the Hessian matrix, i.e., $\partial Q/\partial \lambda_i \partial \lambda_j$, $\partial Q/\partial \alpha_i \partial \alpha_j$, $\partial Q/\partial \lambda_i \partial \alpha_j$, and $\partial Q/\partial \alpha_i \partial \lambda_j$ which consist of the submatrices A, B, C, and D, respectively, as shown in

$$\mathbf{H} = \begin{bmatrix} \mathbf{A} & \mathbf{B} \\ \mathbf{C} & \mathbf{D} \end{bmatrix}. \tag{22}$$

For the submatrix A, the elements are

$$\frac{\partial Q}{\partial \lambda_i \partial \lambda_j} = Q(\boldsymbol{\lambda}, \boldsymbol{\alpha}) \int_X \left(x^{\alpha_i} - M_X^{\alpha_i}\right)\left(x^{\alpha_j} - M_X^{\alpha_j}\right) f_X(x) \mathrm{d}x \tag{23}$$

It is apparent submatrix A is a covariance-like and symmetric one. In a similar way, we have

$$\frac{\partial Q}{\partial \alpha_i \partial \alpha_j} = \alpha_i \alpha_j \lambda_i \lambda_j Q(\boldsymbol{\lambda}, \boldsymbol{\alpha}) \int_X \left(x^{\alpha_i - 1} - M_X^{\alpha_i - 1}\right)\left(x^{\alpha_j - 1} - M_X^{\alpha_j - 1}\right) f_X(x) dx. \tag{24}$$

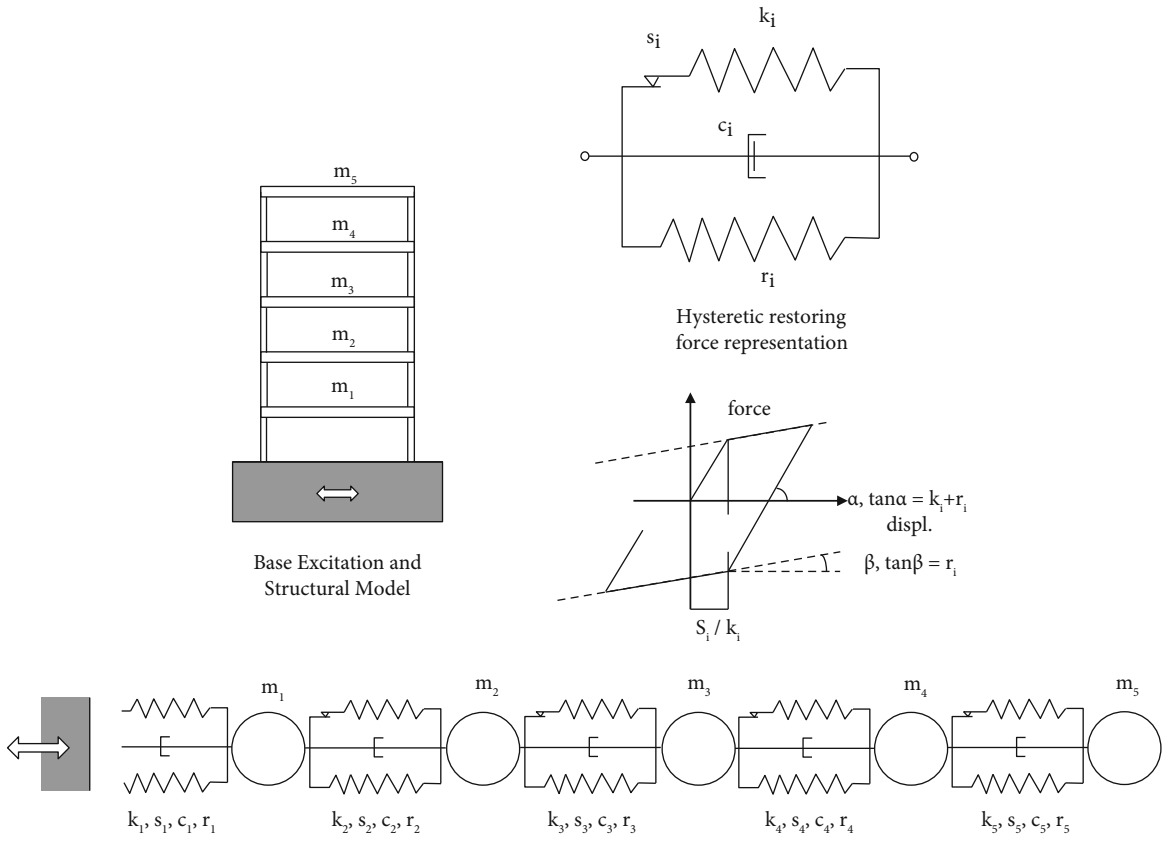

Figure 6: Schematic of a five-story shear building.

Table 4: Means of the random system properties.

Story i	Mass m_i (kg)	Stiffness k_i (N/m)	Stiffness r_i (N/m)	Sliding force stiffness ratio s_i/k_i (m)	Damping ratio ξ_i
1	20×10^3	24×10^6	2.4×10^6	8×10^{-3}	0.06
2	20×10^3	21×10^6	2.1×10^6	8×10^{-3}	0.06
3	20×10^3	18×10^6	1.8×10^6	8×10^{-3}	0.06
4	20×10^3	15×10^6	1.5×10^6	8×10^{-3}	0.06
5	20×10^3	12×10^6	1.2×10^6	8×10^{-3}	0.06

Equation (24) indicates that submatrix D is also a covariance-like and symmetric one. For an element in submatrix B, it has an expression

$$\frac{\partial Q}{\partial \lambda_i \partial \alpha_j} = \alpha_j \lambda_j Q(\boldsymbol{\lambda}, \boldsymbol{\alpha}) \int_X \left(x^{\alpha_i} - M_X^{\alpha_i}\right)\left(x^{\alpha_j - 1} - M_X^{\alpha_j - 1}\right) f_X(x)dx. \tag{25}$$

Similarly, an element in submatrix C has an expression

$$\frac{\partial Q}{\partial \alpha_i \partial \lambda_j} = \alpha_i \lambda_i Q(\boldsymbol{\lambda}, \boldsymbol{\alpha}) \int_X \left(x^{\alpha_i - 1} - M_X^{\alpha_i - 1}\right)\left(x^{\alpha_j} - M_X^{\alpha_j}\right) f_X(x)dx. \tag{26}$$

It can be seen from Equations (25) and (26) that submatrices B and C are also covariance-like ones. An attracting property of submatrices B and C is that the columns of B are the rows of C, i.e., B is the transpose of C.

According to above discussion, the Hessian matrix of $Q(\boldsymbol{\lambda}, \boldsymbol{\alpha})$ is proven to be a covariance-like and symmetric one. As long as the investigated $f_X(x)$ is a PDF, the Hessian matrix is positive definite and of full rank. Thus, the solution to Equation (16) is the minimum point of $Q(\boldsymbol{\lambda}, \boldsymbol{\alpha})$ and furtherly of $I(\boldsymbol{\lambda}, \boldsymbol{\alpha})$. Since the optimization problem in Equation(17), (15) is convex and has no constraint; it seems to provide an opportunity to solve it easily.

4. Computational Issues and Solutions

We have discussed the theoretical rationale of the proposed method in Section 3. However, the technical rationale of the proposed method is more important for implementing this algorithm in practical applications.

4.1. Problem Reformulation. We have proved that the core optimization problem in Equation (17) is a convex one and there is no constraint on it. That is why most of studies have suggested that the optimization procedure can be carried out by the Nelder-Mead algorithm to search the solution $(\lambda_1, \cdots, \lambda_m, \alpha_1, \cdots, \alpha_m)$ [36, 45–50]. However, its technical implementation is not as perfect as the theoretical derivations, based on a lot of numerical implementation experience.

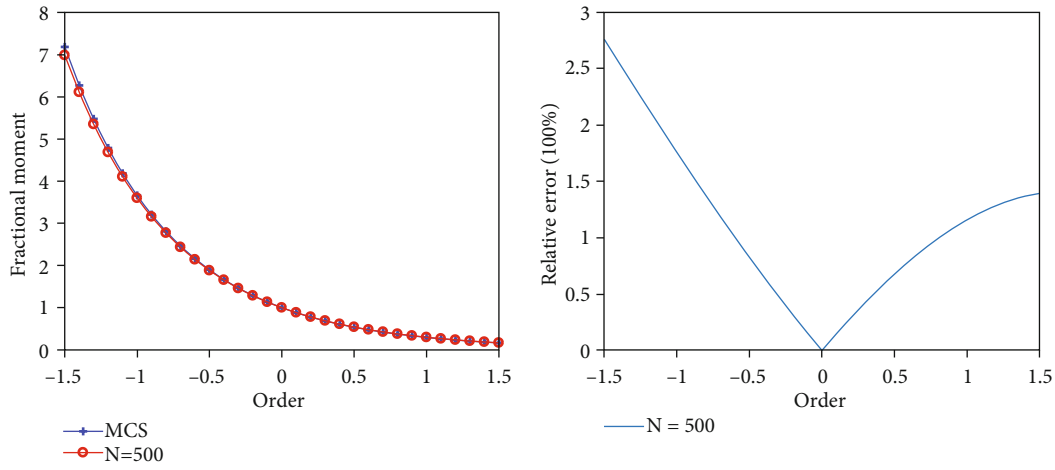

(a) Fractional moment (b) Relative error

Figure 7: Fractional moments and relative error of the normalized response (the nonlinear structural system).

Table 5: The value of the objective function for the nonlinear structure.

	$m = 3$	$m = 4$	$m = 5$
Equation(17)	0.3073	0.3092	0.3108

Table 6: Parameters for the MaxEnt distribution with $m = 3$.

k	0	1	2	3
α_k	0	-0.4950	0.6545	-1.1883
λ_k	7.1554	-14.9265	12.4875	3.0281

The first reason is that the Nelder-Mead algorithm is only suitable for a small number of optimization variables. As the number of optimization variables increases, the performance of the Nelder-Mead algorithm becomes worse. The current study focuses on the high-dimensional time-variant reliability analysis; then, the number of fractional moments is set to be 3 or larger empirically. Thus, the total number of optimization variables is 6 or larger. We also encountered the phenomena of diversity due to different initial values of the optimization variables. This may be caused by the incapability of the Nelder-Mead algorithm.

The second reason is that the estimate error of fractional moment increases with the order of moment, i.e., α [36]. For this reason, the lower-order moments are used in the classical maximum entropy method. To overcome this serious drawback, the values of α should have limits during the optimization procedure. For example, $|\alpha| \leq 2$ was suggested to obtain an unbiased estimation from experimental data [36] and $|\alpha| \leq 1$ was used by Inverardi and Tagliani [42]. In this study, $|\alpha| \leq 1.5$ is used. Additionally, the magnitude of the Lagrange multipliers should also have limits on their values to reduce the searching space and the numerical error associated to the numerical computation. We put the restriction of ±100 on the Lagrange multipliers.

The third reason is the numerical error associated with the integral calculation involved in Equation (17). Furthermore, it affects the accuracy of λ_0, PDF and CDF of the MaxEnt distribution, and further reliability analysis. The CDF of the MaxEnt distribution may be larger than 1 if the improper fractional exponents and Lagrange multipliers are obtained. A high-order global adaptive quadrature is used to perform the integral calculation in this study, which possesses a relatively high accuracy among the numerical integration algorithms in the literature.

Except the above reasons, there is another aspect that is worth to be discussed since it is directly connected with the interval of integration and further the associated accuracy. That is the support of the MaxEnt distribution. Since the samples of structural responses are available when determining the support of the MaxEnt distribution, the maximum, minimum, mean, and standard deviation can be estimated from the samples easily. To avoid arbitrariness, the well-known 6σ principle is suggested to determine the support of the MaxEnt distribution. The upper limit is set to be $x_{\max} + 6s$, where $x_{\max}$ and s are the maximum and standard deviation of the sample, respectively. The lower limit is set to be $x_{\min} - 6s$ if $x_{\min} - 6s$ is larger than 0, where is $x_{\min}$ the minimum observation in the sample. Otherwise, it is set to be 0 as the investigated response quantity has positive support which is required by the definition of fractional moment.

Integrating the above discussion, the reformulated optimization problem has side constraints on the fractional exponents and the Lagrange multipliers. Thus, subset simulation optimization [56, 57] is employed to solve the reformulated optimization problem, instead of the Nelder-Mead algorithm in this study.

4.2. Parameter Estimation Using Subset Simulation Optimization. Subset simulation optimization is a heuristic algorithm for optimization problems, which is extended from a popular reliability method, i.e., subset simulation

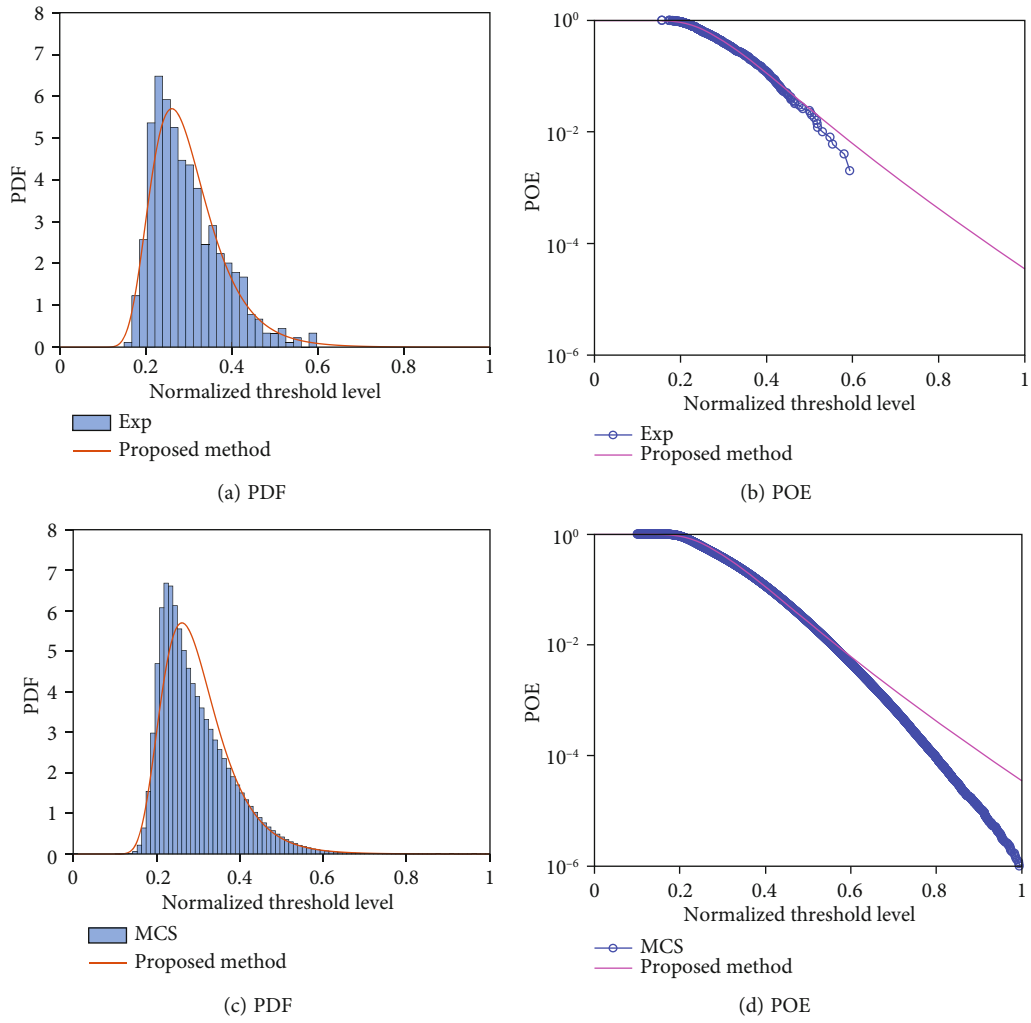

Figure 8: Comparison of histogram, PDF, and POE for the nonlinear structure.

Table 7: The value of the objective function for the nonlinear structure.

$m = 3$	$m = 4$	$m = 5$
44.1	27.9	34.5

[56–58]. An attractive feature of subset simulation optimization is its ability for high-dimensional problems.

Based on the discussion in subsection 4.1, we have reformulated the optimization problem in the MaxEnt principle as an unconstrained one with side constraints on optimization variables. In subset simulation optimization, a truncated normal distribution is assigned to each optimization variable according to the associated side constraint. Take a moment order α_i as an example, the PDF of the corresponding truncated normal distribution is given by [56–58]

$$f_{\alpha_i}(\alpha_i) = \frac{\phi((\alpha_i - \mu_i)/\sigma_i)}{\Phi((\alpha_i^u - \mu_i)/\sigma_i) - \Phi\left((\alpha_i^l - \mu_i)/\sigma_i\right)}, \tag{27}$$

where α_i^u and α_i^l are the upper and lower limits of the moment order, respectively; μ_i and σ_i are the mean value and standard deviation determined by the 3-sigma rule in reliability engineering; and $\phi(\cdot)$ and $\Phi(\cdot)$ are the PDF and cumulative distribution function of standard normal distribution, respectively.

Since the side constraints are considered in the truncated normal distributions, there is no need to handle them during the optimization procedure. Along with the spirit of subset simulation optimization, subsets are generated to approach the optimal solution progressively. All subsets F_i have a generic form as

$$F_i = \{Q(\boldsymbol{\lambda}, \boldsymbol{\alpha}) \le b_i\}, \tag{28}$$

where b_i are the thresholds for the objective function $Q(\boldsymbol{\lambda}, \boldsymbol{\alpha})$ in Equation (17). If one arranges the thresholds in a descent order, i.e., $b_1 \ge b_2 \ge b_3 \cdots$, the subsets have a nested structure

$$F_1 \supset F_2 \supset F_3 \cdots. \tag{29}$$

Thus, the final subset in the sequence would be or include the minimum solution theoretically.

In subset simulation optimization, the value of the objective function $Q(\boldsymbol{\lambda}, \boldsymbol{\alpha})$ is the driving quantity for optimization, while the optimization procedure is achieved by the evaluation of the level probability p_i that is an optimization parameter for subset simulation optimization. The conditional probability between two contiguous subsets is defined as the level probability and simulated by Markov Chain Monte Carlo simulation, i.e.,

$$p_i = P(F_{i+1}|F_i) \approx \frac{1}{M}\sum_{i=}^{M} I[Q(\boldsymbol{\lambda}, \boldsymbol{\alpha}) \geq b_{i+1}], \tag{30}$$

where M is the number of candidate designs (or samples) belonging to the subset F_i, and $I(\cdot)$ is an indicator function which is used to check a candidate design falling in F_{i+1} or not. In this study, we adopted a strategy in which the value of p_k is reduced as the number of optimization iterations (or simulation level) increases.

The standard deviation of the samples in the $(i+1)$th simulation level is employed to check the convergence of the optimal searching. The estimator of standard deviation tends to zero while the searching process is approaching the global minimum. At the same time, we also impose a maximum number of simulation levels as another stopping criterion to avoid the overflow of the affordable computational effort.

More details of subset simulation optimization can be referred to Refs. [56–58].

5. Test Problems

Two dynamic reliability analysis problems are used to demonstrate the performance of the proposed method. The first problem involves a single-degree-of-freedom (SDOF) oscillator which has a linear behavior, while the second problem is a five-DOF structural system with nonlinear behavior.

5.1. A SDOF Oscillator. The investigated SDOF oscillator is shown in Figure 2 with a white noise excitation $W(t)$. The governing equation of this structural system is given by

$$\ddot{Y}(t) + 2\varsigma\omega Y(t) + \omega^2 Y(t) = W(t), \tag{31}$$

where the natural frequency is = 7.85rad/s (1.25Hz) and the damping ratio is $\varsigma = 2\%$, respectively. The spectral intensity of the white noise S takes 1. The following initial conditions are applied to the system:

$$\begin{cases} Y(0) = 0, \\ \dot{Y}(0) = 0. \end{cases} \tag{32}$$

The failure event of this system is defined as its maximum displacement exceeding a threshold $b = 2.1$ over a time interval $[0, 30]$ s

$$F = \left\{ \max_{k=1,\cdots,n} |Y(t_k)| > b \right\}, \tag{33}$$

where n is the total number of discrete time instants to represent the Gaussian white noise. Ref. [33] used a constant time step size $\Delta t = 0.002$s for discretizing the time interval of interest, which leads to the total number of time instants be $n = 30/\Delta t + 1 = 1501$. Then, 1501 input standard normal random variables φ_k are employed to represent the input white noise, i.e.,

$$\left\{ W(t_k) = \sqrt{\frac{2\pi S}{\Delta t}}\varphi_k : k = 1, \cdots, n \right\}. \tag{34}$$

To meet the definition of the fractional moment, the structural response associated to the failure event in Equation (33) is rewritten as

$$G_n = g_n(\mathbf{X}, \mathbf{Y}(t), t) = \frac{\max_{k=1,\cdots,n} |Y(t_k)|}{b}, \tag{35}$$

where G_n is the normalized structural response. Then, the proposed method was applied to solve this problem with a sample size $N = 500$, 1000, 1500, and 2000. For the purpose of comparison, an MCS with 10^6 samples was carried out to obtain a reference result.

Figure 3 shows the comparisons of the fractional moments and the relative error for the normalized response in Equation (35). Here, the order of fractional moments varies in the interval of $[-1.5, 1.5]$ as we discussed in Section 4.1. The fractional moments calculated from different sample sizes almost overlap one another (Figure 3(a)). However, it is clear that the relative error is becoming small with the increase of sample size N (Figure 3(b)). Furthermore, the biggest relative error is 1% when the order of fractional moment takes -1.5, which is close to the used values reported by Xu and Wang [48] using a low-discrepancy sequence. Therefore, the relatively accurate fractional moments are employed in the proposed method by limiting the scale of the order exponents.

Inverardi and Tagliani proposed a penalty term m/N, which is proportional to the order of the MaxEnt distribution m and inversely proportional to the sample size N, to avoid reconstructing a "too elaborate" distribution that cannot be justified by the given experimental data [42]. Table 1 lists the values of the objective function in Equation (17) while Table 2 gives the values of the objective function considering the penalty term. Six digitals must be kept in order to observe the difference among the results for a sample size in Table 1, while four digitals are required in Table 2. The value of the objective function increases as the number of fractional moments used in the MaxEnt distribution and decreases with the number of samples adopted for the estimation of fractional moments. Thus, $m = 3$ is preferable for approximating the MaxEnt distribution of the normalized structural response, and 2000 samples provide the most

accurate estimation of fractional moment and further reduce the objective function value.

Figures 4 and 5 show the histograms, PDFs, and probability of exceedances (POEs) [36] obtained by the proposed method and MCS. Since all settings of parameters produce very similarly results, we only report the results for $m = 3$ with $N = 500$ (Figure 4) and 2000 (Figure 5). The term "Exp" refers to the experimental data (sample) used to estimate the fractional moments. The results of the proposed method agree with those of MCS, low to a very small probability (about 10^{-6}). Thus, the proposed method possesses a good accuracy and efficiency for this investigated linear system.

We completed all calculations on a desktop PC with CPU@3.60 GHz and 16 GB RAM. Table 3 reports the average computational time of the SDOF oscillator based on 30 runs of different combinations of N and m. Although it is hard to draw a common conclusion from these data, the average calculational time that are around 20~ 40 s is attractive for engineering optimization design.

5.2. A Nonlinear Five-DOF Structural System. The second example is a five-DOF shear building adapted from Refs. [34, 51]. The structural system shown in Figure 6 is subjected to an external excitation. There are 25 input random variables to model uncertainties in the system properties, including masses, stiffness, sliding force stiffness ratios, and damping ratios. Table 4 lists the means of these 25 input random variables which are independently and normally distributed. Note that the damping terms c_i in are given by

$$c_i = 2\xi_i \sqrt{m_i(k_i + r_i)}, \tag{36}$$

where ξ_i are the damping ratios, m_i are the masses, and $k_i + r_i$ are the stiffness, respectively. Except for the damping variables, the coefficient of variation of the other random property variables is set to be 0.1. The standard deviations of damping variables are set to be 0.01.

Suppose that the external excitation to the structural system is a general Gaussian excitation acting on the horizontal ground. The Karhunen-Loève expansion is used to represent it with 200 independent standard normal variables. Therefore, there are total 225 input random variables which are beyond the capacity of FORM and surrogate model methods.

The failure event is defined by the first-passage of the maximum displacement at the first story with a threshold $b = 0.039$m For the structural dynamic analysis, the time interval of $[0.0\,\text{s}, 20.0\,\text{s}]$ is discretized by a time step size of 0.01 s.

For this problem, 500 experimental points generated from MCS are employed to estimate the fractional moments of the normalized response. The comparisons of fractional moments and the corresponding relative errors are shown in Figure 7. Similar conclusions can be drawn as for the SDOF oscillator, except that the magnitude of relative error grows to 2.75% for $\alpha = -1.5$.

Additionally, $m = 3$, 4, and 5 are adopted in the proposed method. Table 5 lists the values of the objective function with penalty term. As the value of m increases, the values of the objective function also increase, which is consistent with the results of the SDOF oscillator. This indicates that the MaxEnt distribution with $m = 3$ has a good balance of accuracy and model complexity. Table 6 lists the orders of fractional moments and Lagrange multipliers obtained by the proposed method.

Based on the parameters in Table 6, we reconstructed the distribution of the normalized response and compared the proposed method and MCS in Figure 8. The PDF curve of the proposed method matches the histogram of the experimental data closely (Figure 8(a)), while we observed a dispersion between it and the histogram of MCS samples in Figure 8(c). Similarly, the POE curve of the proposed method agrees with that of experimental data (Figure 8(b)), whereas it has a deviation from the curve estimated from MCS samples (Figure 8(d)). For the interval of $[10^{-3}, 10^{0}]$, the POE of the proposed method has a good agreement with that of MCS. The failure probability is estimated as 1.3400×10^{-6} by MCS with 10^7 samples when the threshold level b is 0.039 m (corresponding to the case of the normalized threshold level of 1). The estimation of failure probability yielded by the proposed method is 3.5027×10^{-5}. Therefore, the proposed method overestimated the failure probability for a large threshold level. Compared with the investigated linear system, the overestimations may cause by the nonlinear behavior of the current structural system.

Table 7 reports the average computational time of the nonlinear structural system based on 30 runs of different m. Similar conclusion can be drawn from this table as that of the SDOF oscillator example.

6. Conclusions

In this study, a maximum entropy distribution method is proposed to perform structural reliability analysis for high-dimensional problems with random process input. With the development of the maximum entropy distribution with fractional moments, we proved that the solution to a function $Q(\boldsymbol{\lambda}, \boldsymbol{\alpha})$ is the global one to the maximum relative entropy between the true PDF and the approximate one. Thus, the corresponding optimization problem is converted into a convex one with a global solution. To estimate the fractional moments efficiently, a set of experimental points are generated for this purpose, which provides the estimator of a fractional moment for any order. Converting the common optimization problem into an equivalent one can avoid the trapping in a locally optimal solution. Furthermore, we reexamined the associated computational issues of the target optimization problem and reformulated it with side constraints on the optimization variables, i.e., the orders of fractional moments and the corresponding Lagrange multipliers. Subset simulation optimization is used to solve the new optimization problem.

Two benchmark problems with high-dimensional inputs show that the proposed method has both good accuracy and efficiency. If the limit state function, however, has a strong nonlinear behavior with respect to inputs, the maximum

entropy distribution may not approximate the tail region accurately, and in this case, the proposed method may result in a low efficiency or accuracy, or both.

Future studies will involve developing efficiently sampling methods for the estimation of fractional moments for high-dimensional nonlinear problems.

Appendix

A. Symbols

$g(\cdot)$:limit state function
G, G_i:response quantity and its value given an input
X, x:input random variables and its observation
$\mathbf{X}$,$\mathbf{x}$:random vector and its observation vector
$\mathbf{Y}(t)$:input random process vector
t,t_f:time and final time
$R(\cdot)$:reliability function
$P_f(\cdot)$:failure probability function
Δt:time step
$\mathbf{Z}$:random vector transformed from input random process
Pr $(\cdot)$:probability operator
$E(\cdot)$:expectation operator
W:maximum value variable
α, α_i:order of fractional moment
$f_X(x)$,$\widehat{f}_X(x)$:probability density function and approximate probability density function
c:reference point
M_x^α:αth fractional moment
λ_i:Lagrange multiplier
$\mathbf{I}(\cdot)$:objective function
$Q(\cdot)$:potential function
$\mathbf{A}$, $\mathbf{B}$, $\mathbf{C}$ and $\mathbf{D}$ submatrix

B.

Recall that the PDF of MaxEnt distribution is given by

$$\widehat{f}_X(x) = \exp(-\lambda_0)\exp\left(-\sum_{i=1}^{m}\lambda_i x^{\alpha_i}\right). \tag{B.1}$$

Since $\int f_X(x)dx = 1$, one could obtain the following relationship:

$$\exp(-\lambda_0) = \frac{1}{\int \exp\left(-\sum_{i=1}^{m}\lambda_i x^{\alpha_i}\right)dx}. \tag{B.2}$$

Substitute Equation (B.2) into Equation (B.1), the PDF expression of MaxEnt distribution is

$$\widehat{f}_X(x) = \frac{\exp\left(-\sum_{i=1}^{m}\lambda_i x^{\alpha_i}\right)}{\int \exp\left(-\sum_{i=1}^{m}\lambda_i x^{\alpha_i}\right)dx}. \tag{B.3}$$

Further, the PDF expression of MaxEnt distribution can be rewritten as

$$\begin{aligned}\widehat{f}_X(x) &= \frac{\exp\left(\sum_{i=1}^{m}\lambda_i M_X^{\alpha_i}\right)\cdot\exp\left(-\sum_{i=1}^{m}\lambda_i x^{\alpha_i}\right)}{\exp\left(\sum_{i=1}^{m}\lambda_i M_X^{\alpha_i}\right)\cdot\int\exp\left(-\sum_{i=1}^{m}\lambda_i x^{\alpha_i}\right)dx}\\ &= \frac{\exp\left(-\sum_{i=1}^{m}\lambda_i\left(x^{\alpha_i}-M_X^{\alpha_i}\right)\right)}{\int\exp\left(-\left(x^{\alpha_i}-M_X^{\alpha_i}\right)\right)dx},\end{aligned} \tag{B.4}$$

as long as $\exp\left(\sum_{i=1}^{m}\lambda_i M_X^{\alpha_i}\right) \neq 0$. With the definition of $Q(\boldsymbol{\lambda}, \boldsymbol{\alpha})$ in Equation (17), one obtain that

$$\widehat{f}(x) = [Q(\boldsymbol{\lambda}, \boldsymbol{\alpha})]^{-1}\exp\left(-\sum_{i=1}^{m}\lambda_i\left(x^{\alpha_i}-M_X^{\alpha_i}\right)\right). \tag{B.5}$$

Data Availability

Some or all data, models, or code generated or used during the study are available from the corresponding author by request.

Conflicts of Interest

The authors declare that they have no conflicts of interest.

References

[1] R. Rackwitz and B. Flessler, "Structural reliability under combined random load sequences," *Computers & Structures*, vol. 9, no. 5, pp. 489–494, 1978.

[2] K. Breitung, "Asymptotic approximations for probability integrals," *Probabilistic Engineering Mechanics*, vol. 4, no. 4, pp. 187–190, 1989.

[3] X. Du and Z. Hu, "First order reliability method with truncated random variables," *Journal of Mechanical Design*, vol. 134, no. 9, article 091005, 2012.

[4] Y.-G. Zhao and T. Ono, "Moment methods for structural reliability," *Structural Safety*, vol. 23, no. 1, pp. 47–75, 2001.

[5] Y.-G. Zhao and T. Ono, "On the problems of the fourth moment method," *Structural Safety*, vol. 26, no. 3, pp. 343–347, 2004.

[6] C. G. Bucher and U. Bourgund, "A fast and efficient response surface approach for structural reliability problems," *Structural Safety*, vol. 7, no. 1, pp. 57–66, 1990.

[7] M. R. Rajashekhar and B. R. Ellingwood, "A new look at the response surface approach for reliability analysis," *Structural Safety*, vol. 12, no. 3, pp. 205–220, 1993.

[8] H. P. Gavin and S. C. Yau, "High-order limit state functions in the response surface method for structural reliability analysis," *Structural Safety*, vol. 30, no. 2, pp. 162–179, 2008.

[9] H. S. Li, Z. Z. Lu, and H. W. Qiao, "A new high-order response surface method for structural reliability analysis," *Structural Engineering and Mechanics*, vol. 34, no. 6, pp. 779–799, 2010.

[10] R. E. Melchers, "Importance sampling in structural systems," *Structural Safety*, vol. 6, no. 1, pp. 3–10, 1989.

[11] S. K. Au and J. L. Beck, "A new adaptive importance sampling scheme for reliability calculations," *Structural Safety*, vol. 21, no. 2, pp. 135–158, 1999.

[12] P. H. Madsen and S. Krenk, "An integral equation method for the first-passage problem in random vibration," *Journal of Applied Mechanics*, vol. 51, no. 3, pp. 674–679, 1984.

[13] Ø. Hagen and L. Tvedt, "Vector process out-crossing as parallel system sensitivity measure," *Journal of Engineering Mechanics*, vol. 117, no. 10, pp. 2201–2220, 1991.

[14] C. Andrieu-Renaud, B. Sudret, and M. Lemaire, "The PHI2 method: a way to compute time-variant reliability," *Reliability Engineering & System Safety*, vol. 84, no. 1, pp. 75–86, 2004.

[15] B. Sudret, "Analytical derivation of the outcrossing rate in time-variant reliability problems," *Structure and Infrastructure Engineering*, vol. 4, no. 5, pp. 353–362, 2008.

[16] J. Zhang and X. Du, "Time-dependent reliability analysis for function generator mechanisms," *Journal of Mechanical Design*, vol. 133, no. 3, article 031005, 2011.

[17] Z. Hu and X. Du, "Time-dependent reliability analysis with joint upcrossing rates," *Structural and Multidisciplinary Optimization*, vol. 48, no. 5, pp. 893–907, 2013.

[18] Z. Hu, H. Li, X. du, and K. Chandrashekhara, "Simulation-based time-dependent reliability analysis for composite hydrokinetic turbine blades," *Structural and Multidisciplinary Optimization*, vol. 47, no. 5, pp. 765–781, 2013.

[19] J.-B. Chen and J. Li, "The extreme value distribution and dynamic reliability analysis of nonlinear structures with uncertain parameters," *Structural Safety*, vol. 29, no. 2, pp. 77–93, 2007.

[20] J. Li, J.-B. Chen, and W.-L. Fan, "The equivalent extreme-value event and evaluation of the structural system reliability," *Structural Safety*, vol. 29, no. 2, pp. 112–131, 2007.

[21] Z. Wang and P. Wang, "A nested extreme response surface approach for time-dependent reliability-based design optimization," *Journal of Mechanical Design*, vol. 134, no. 12, article 121007, 2012.

[22] Z. Hu and X. Du, "A sampling approach to extreme value distribution for time-dependent reliability analysis," *Journal of Mechanical Design*, vol. 135, no. 7, article 071003, 2013.

[23] Z. Wang and P. Wang, "A double-loop adaptive sampling approach for sensitivity-free dynamic reliability analysis," *Reliability Engineering & System Safety*, vol. 142, pp. 346–356, 2015.

[24] Z. Hu and S. Mahadevan, "A single-loop kriging surrogate modeling for time-dependent reliability analysis," *Journal of Mechanical Design*, vol. 138, no. 6, article 061406, 2016.

[25] Z. Wang and W. Chen, "Confidence-based adaptive extreme response surface for time-variant reliability analysis under random excitation," *Structural Safety*, vol. 64, pp. 76–86, 2017.

[26] Z. Hu and X. Du, "Mixed efficient global optimization for time-dependent reliability analysis," *Journal of Mechanical Design*, vol. 137, no. 5, article 051401, 2015.

[27] D. Zhang, X. Han, C. Jiang, J. Liu, and Q. Li, "Time-dependent reliability analysis through response surface method," *Journal of Mechanical Design*, vol. 139, no. 4, article 041404, 2017.

[28] A. Singh, Z. P. Mourelatos, and J. Li, "Design for lifecycle cost using time-dependent reliability," *Journal of Mechanical Design*, vol. 132, no. 9, article 091008, 2010.

[29] Z. P. Mourelatos, M. Majcher, V. Pandey, and I. Baseski, "Time-dependent reliability analysis using the total probability theorem," *Journal of Mechanical Design*, vol. 137, no. 3, article 031405, 2015.

[30] G. J. Savage and Y. K. Son, "Dependability-based design optimization of degrading engineering systems," *Journal of Mechanical Design*, vol. 131, no. 1, article 011002, 2009.

[31] Y. K. Son and G. J. Savage, "Set theoretic formulation of performance reliability of multiple response time-variant systems due to degradations in system components," *Quality and Reliability Engineering International*, vol. 23, no. 2, pp. 171–188, 2007.

[32] C. Jiang, X. P. Huang, X. Han, and D. Q. Zhang, "A time-variant reliability analysis method based on stochastic process discretization," *Journal of Mechanical Design*, vol. 136, no. 9, article 091009, 2014.

[33] S.-K. Au and J. L. Beck, "Estimation of small failure probabilities in high dimensions by subset simulation," *Probabilistic Engineering Mechanics*, vol. 16, no. 4, pp. 263–277, 2001.

[34] S. K. Au, J. Ching, and J. L. Beck, "Application of subset simulation methods to reliability benchmark problems," *Structural Safety*, vol. 29, no. 3, pp. 183–193, 2007.

[35] M. G. Kendall, A. Stuart, and J. K. Ord, *Kendall's Advanced Theory of Statistics*, vol. 1, Charles Griffin & Company Ltd, 1987.

[36] X. Zhang and M. D. Pandey, "Structural reliability analysis based on the concepts of entropy, fractional moment and dimensional reduction method," *Structural Safety*, vol. 43, pp. 28–40, 2013.

[37] G. Li and K. Zhang, "A combined reliability analysis approach with dimension reduction method and maximum entropy method," *Structural and Multidisciplinary Optimization*, vol. 43, no. 1, pp. 121–134, 2011.

[38] E. T. Jaynes, "Information theory and statistical mechanics," *Physical Review*, vol. 106, no. 4, pp. 620–630, 1957.

[39] E. T. Jaynes, *Probability Theory: The Logic of Science*, Cambridge Univeristy Press, Cambridge, UK, 2003.

[40] S. Rahman and H. Xu, "A univariate dimension-reduction method for multi-dimensional integration in stochastic mechanics," *Probabilistic Engineering Mechanics*, vol. 19, no. 4, pp. 393–408, 2004.

[41] H. Xu and S. Rahman, "A generalized dimension-reduction method for multidimensional integration in stochastic mechanics," *International Journal for Numerical Methods in Engineering*, vol. 61, no. 12, pp. 1992–2019, 2004.

[42] P. L. N. Inverardi and A. Tagliani, "Maximum entropy density estimation from fractional moments," *Communications in Statistics - Theory and Methods*, vol. 32, no. 2, pp. 327–345, 2003.

[43] B. Li, L. Zhang, X. Zhu, X. Yu, and X. Ma, "Reliability analysis based on a novel density estimation method for structures with correlations," *Chinese Journal of Aeronautics*, vol. 30, no. 3, pp. 1021–1030, 2017.

[44] H. Dai, H. Zhang, and W. Wang, "A new maximum entropy-based importance sampling for reliability analysis," *Structural Safety*, vol. 63, pp. 71–80, 2016.

[45] Y. Shi, Z. Lu, K. Cheng, and Y. Zhou, "Temporal and spatial multi-parameter dynamic reliability and global reliability sensitivity analysis based on the extreme value moments," *Structural and Multidisciplinary Optimization*, vol. 56, no. 1, pp. 117–129, 2017.

[46] J. Xu, "A new method for reliability assessment of structural dynamic systems with random parameters," *Structural Safety*, vol. 60, pp. 130–143, 2016.

[47] J. Xu, C. Dang, and F. Kong, "Efficient reliability analysis of structures with the rotational quasi- symmetric point- and the maximum entropy methods," *Mechanical Systems and Signal Processing*, vol. 95, pp. 58–76, 2017.

[48] J. Xu and D. Wang, "A two-step methodology to apply low-discrepancy sequences in reliability assessment of structural dynamic systems," *Structural and Multidisciplinary Optimization*, vol. 57, no. 4, pp. 1643–1662, 2018.

[49] J. Xu, D. Wang, and C. Dang, "A marginal fractional moments based strategy for points selection in seismic response analysis of nonlinear structures with uncertain parameters," *Journal of Sound and Vibration*, vol. 387, pp. 226–238, 2017.

[50] J. Xu, W. Zhang, and R. Sun, "Efficient reliability assessment of structural dynamic systems with unequal weighted quasi-Monte Carlo simulation," *Computers and Structures*, vol. 175, pp. 37–51, 2016.

[51] G. I. Schuëller and H. J. Pradlwarter, "Benchmark study on reliability estimation in higher dimensions of structural systems - an overview," *Structural Safety*, vol. 29, no. 3, pp. 167–182, 2007.

[52] Z. Li, F. Nie, X. Chang, L. Nie, H. Zhang, and Y. Yang, "Rank-constrained spectral clustering with flexible embedding," *IEEE Transactions on Neural Networks and Learning Systems*, vol. 29, no. 12, pp. 6073–6082, 2018.

[53] Z. Li, F. Nie, X. Chang, Y. Yang, C. Zhang, and N. Sebe, "Dynamic affinity graph construction for spectral clustering using multiple features," *IEEE Transactions on Neural Networks and Learning Systems*, vol. 29, no. 12, pp. 6323–6332, 2018.

[54] Z. Li, L. Yao, X. Chang, K. Zhan, J. Sun, and H. Zhang, "Zero-shot event detection via event-adaptive concept relevance mining," *Pattern Recognition*, vol. 88, pp. 595–603, 2019.

[55] H. Gzyl and A. Tagliani, "Hausdorff moment problem and fractional moments," *Applied Mathematics and Computation*, vol. 216, no. 11, pp. 3319–3328, 2010.

[56] H.-S. Li, "Subset simulation for unconstrained global optimization," *Applied Mathematical Modelling*, vol. 35, no. 10, pp. 5108–5120, 2011.

[57] H.-S. Li and Z.-J. Cao, "Matlab codes of subset simulation for reliability analysis and structural optimization," *Structural and Multidisciplinary Optimization*, vol. 54, no. 2, pp. 391–410, 2016.

[58] H.-S. Li and S.-K. Au, "Design optimization using subset simulation algorithm," *Structural Safety*, vol. 32, no. 6, pp. 384–392, 2010.